

Charge Disproportionation in $R\text{NiO}_3$ Perovskites: Simultaneous Metal-Insulator and Structural Transition in YNiO_3

J. A. Alonso,¹ J. L. García-Muñoz,² M. T. Fernández-Díaz,³ M. A. G. Aranda,⁴ M. J. Martínez-Lope,¹ and M. T. Casais¹

¹*Instituto de Ciencia de Materiales de Madrid, CSIC, Cantoblanco, E-28049 Madrid, Spain*

²*Institut de Ciència de Materials de Barcelona, CSIC, Campus UAB, Bellaterra, E-08193 Barcelona, Spain*

³*Institut Laue-Langevin, BP 156, 38042 Grenoble Cedex 9, France*

⁴*Departamento de Química Inorgánica, Cristalografía y Mineralogía, Facultad de Ciencias, Universidad de Málaga, E-29071 Málaga, Spain*

(Received 16 October 1998)

Neutron and synchrotron diffraction data provide the first observation of changes in the crystal symmetry at the metal-insulator transition in $R\text{NiO}_3$ perovskites. At high temperatures, YNiO_3 is orthorhombic and metallic but below $T_{\text{MI}} = 582$ K it changes to a monoclinic insulator due to a charge disproportionation ($2\text{Ni}^{3+} \rightarrow \text{Ni}^{3+\delta} + \text{Ni}^{3-\delta}$) that develops at the opening of the gap. We report the presence of two alternating NiO_6 octahedra with expanded (Ni1) and contracted (Ni2) Ni-O bonds and a magnetic structure [$\mathbf{k} = (1/2, 0, 1/2)$] with unequal moments at Ni1 and Ni2 octahedra. [S0031-9007(99)09077-8]

PACS numbers: 71.30.+h, 71.45.Lr, 71.38.+i, 75.25.+z

One of the long-standing questions associated with $R\text{NiO}_3$ perovskites (R = rare earth) is the origin of the first order metal-insulator transition and the nature of their insulating state [1–9]. The current scenario for the transition suggests that the closing of the Ni-O-Ni angle (θ) by thermal contraction when temperature decreases reduces the $3d$ - $2p$ - $3d$ orbital overlap beyond its critical value producing a gap opening [2,3]. Conversely with the isostructural $R\text{MnO}_3$ oxides (believed to be of the Mott-Hubbard class in the framework developed by Zaanen, Sawatzky, and Allen [10]) the rare earth nickelates are probably at the boundary between “low- Δ metals” and “charge-transfer” insulators (Δ , charge transfer energy). When electronic localization occurs, an isotropic expansion of the Ni-O bonds ($\Delta d_{\text{Ni-O}} \approx +0.004$ Å) has been reported in Pr, Nd, and Sm nickelates [3] that accounts for the observed volume expansion of $\Delta V/V \approx 0.25\%$ ($M \rightarrow I$). Ni^{3+} ($t_{2g}^6 e_g^1$) as well as Mn^{3+} ($t_{2g}^3 e_g^1$) are Jahn-Teller ions with a single e_g electron with orbital degeneracy. In stoichiometric $R\text{MnO}_{3,00}$ oxides static Jahn-Teller deformations break down the twofold degeneracy of the e_g orbitals stabilizing a layered antiferromagnetic (AFM) structure. In contrast the NiO_6 octahedra are very regular in all the investigated Ni perovskites, probably as a manifestation of the higher covalent character of the Ni oxides. Moreover, based on the discovery of an unprecedented magnetic ordering of $S = \frac{1}{2}$ Ni moments in PrNiO_3 and NdNiO_3 , a nonuniform orbital occupancy of the single e_g electron in the low-spin Ni^{3+} ($t_{2g}^6 e_g^1$) configuration was predicted [8,9]. In the insulating state, the magnetic structure is characterized by an unexpected propagation vector $\mathbf{k} = (\frac{1}{2}, 0, \frac{1}{2})$. This magnetic symmetry is not compatible with nearest-neighbor (NN) exchange coupling of the same sign and requires alternating ferromagnetic (FM) and AFM Ni-O-Ni couplings along the three pseudocubic axis. This can be achieved if there

is a $d_{x^2-y^2}/d_{z^2}$ -orbital ordering that breaks down the inversion center at the Ni site in the orthorhombic symmetry [8]. Nevertheless, the structural distortion from such orbital ordering has so far not been observed.

More recently, the scenario has changed after the observation of very large positive ^{16}O - ^{18}O isotope shifts in the metal-insulator (MI) transition temperatures of $R\text{NiO}_3$ with Pr, Nd, Sm, and Eu [11]. These results establish the importance of the electron-lattice coupling for the MI transition and suggest the presence of Jahn-Teller polarons.

We have investigated the very distorted YNiO_3 perovskite in an attempt to enhance the electron-lattice coupling. The previously investigated $R\text{NiO}_3$ oxides (R = Pr, Nd, Sm, and Eu) have the perovskite-distorted GdFeO_3 structure ($Pbnm$) and exhibit MI transitions at, respectively, 130 K (Pr), 200 K (Nd), 400 K (Sm), and 460 K (Eu) [2–4]. For Pr and Nd $T_N = T_{\text{MI}}$ but the difference between the magnetic (T_N) and the MI transitions systematically increases when the size of R is reduced ($T_N < T_{\text{MI}}$). The difficulties found in the synthesis, inherent to the stabilization of Ni^{3+} cations, are more severe for smaller rare earths. We have been able to prepare YNiO_3 in a piston-cylinder press [12]; this sample had not been prepared within the last 25 years [13], and nothing was known about its structure, magnetism, or metal-insulator transition. Synchrotron and neutron experiments on polycrystalline YNiO_3 were performed at the European Synchrotron Radiation Facility and the Institut Laue Langevin (ILL) in Grenoble. Synchrotron x-ray diffraction (SXRD) patterns were collected at the BM16 high resolution powder diffractometer using a short wavelength of $\lambda = 0.518056(3)$ Å. Eleven patterns were collected across the MI transition, previously characterized by differential scanning calorimetry measurements. A room temperature (RT) neutron powder diffraction

(NPD) pattern was collected at the D2B high resolution diffractometer of the ILL, using a wavelength of 1.594 Å. The magnetic intensities were obtained from the low-temperature NPD patterns collected with $\lambda = 2.52$ Å at the D1B diffractometer. The data were analyzed by the Rietveld method, using the GSAS [14] and FULLPROF [15] programs.

The inset of Fig. 1 illustrates the DSC curves for YNiO_3 obtained during heating and cooling runs. The heating (cooling) run exhibits an endothermic (exothermic) peak corresponding to the insulator-to-metal transition at 582.1 (579.2) K. In the heating process the entropy gain is associated with the electronic delocalization entering the metallic state and the concomitant structural change. The SXRD patterns of YNiO_3 above T_{MI} could be refined in the conventional $Pbnm$ orthorhombic symmetry [16]. However, a close examination of the high-resolution SXRD profiles below T_{MI} showed a clear splitting of some reflections, characteristic of a monoclinic structural distortion. This is illustrated in Fig. 2, where the orthorhombic (224) reflection, single above T_{MI} , splits into the separated monoclinic reflections (224) and (22-4), confirming a lowering of crystallographic symmetry. Below T_{MI} the structure of YNiO_3 was successfully refined in the monoclinic $P2_1/n$ space group from SXRD data. Figure 1(a) shows the temperature variation of unit-cell parameters of YNiO_3 across the transition. Conversely with less distorted members of the RNiO_3 family (for which $\Delta b/b = 0.11\% - 0.14\%$), the b parameter contracts at T_{MI} ($\Delta b/b = -0.16\%$). As a consequence the relative volume expansion

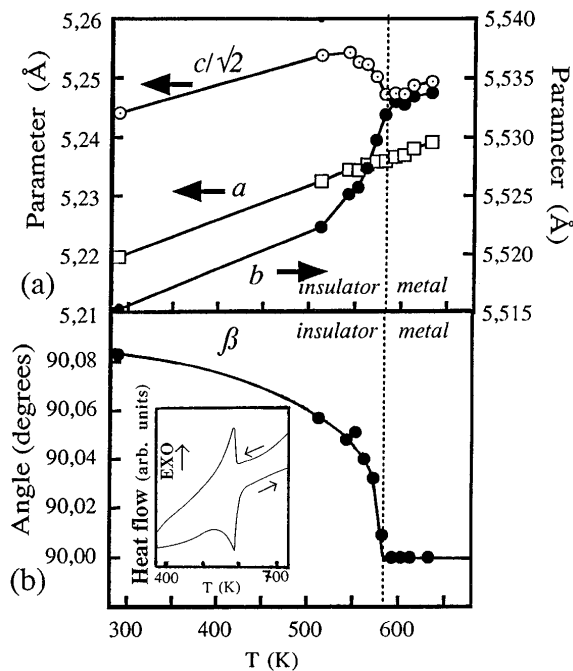


FIG. 1. Temperature dependence of (a) the cell edges and (b) the monoclinic β angle across the metal-insulator transition in YNiO_3 . Inset: DSC curves obtained on heating and cooling runs.

($\Delta V/V = 0.10\%$ for Y) is approximately half of that found for Pr, Nd, or Sm ($\Delta V/V = 0.20\% - 0.25\%$). Below the transition, the deviation from 90° of the monoclinic angle β is illustrated in Fig. 1(b). These results represent the first observation of a modification of the crystallographic symmetry concomitant with the electronic localization in Ni perovskites.

It is interesting to note that in the $P2_1/n$ symmetry there are two crystallographically independent Ni positions (Ni1 and Ni2), as well as three nonequivalent oxygen atoms (O1, O2, and O3) all in general (x, y, z) positions. A simultaneous refinement of the SXRD and NPD data taken at RT allowed us to obtain very accurate oxygen positions for the monoclinic phase, listed in Table I. In Fig. 3 we have represented the octahedral oxygen coordination around Ni1 and Ni2 atoms, which alternate along the three directions of the crystal. The most remarkable finding is that the monoclinic symmetry is a consequence of very significant differences in the average size of both kind of octahedra. The mean Ni-O distance in the NiO_6 octahedron is 1.994(3) Å, to be compared with the shorter value of 1.923(3) Å in Ni_2O_6 .

In other members of the family with small-size rare earths we confirmed that the monoclinic splitting increases as R size decreases. In addition, it is found that the

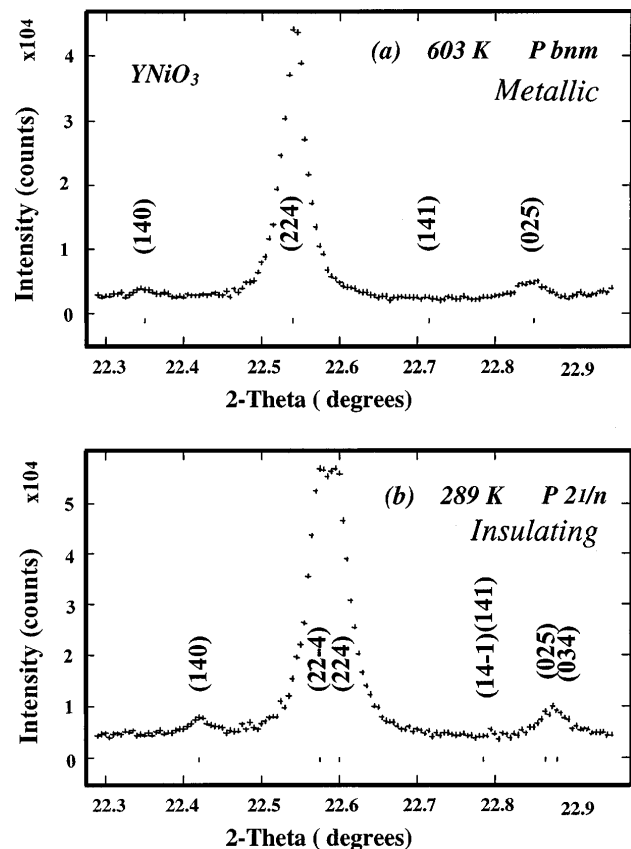


FIG. 2. Selected raw synchrotron x-ray diffraction patterns showing the splitting of the orthorhombic (224) reflection in (224) and (22-4) peaks due to the monoclinic distortion below T_{MI} .

TABLE I. Atomic parameters for YNiO_3 at RT, from combined SXR and NPD data. Space group $P2_1/n$, $a = 5.17932(5)$, $b = 5.51529(5)$, $c = 7.41656(7)$ Å, $\beta = 90.081(1)^\circ$.

Atom	Site	x	y	z	B (Å ²)
Y	4e	0.9816(2)	0.0729(1)	0.2502(4)	0.52(2)
Ni1	2d	0.5	0	0	0.55(5)
Ni2	2c	0.5	0	0.5	0.28(5)
O1	4e	0.0998(3)	0.4705(3)	0.2457(5)	0.54(4)
O2	4e	0.6973(7)	0.3080(7)	0.0467(5)	0.55(6)
O3	4e	0.1882(6)	0.2038(7)	0.9465(5)	0.57(7)

distortion parameter of NiO_6 octahedra, $\Delta_d = (\frac{1}{6}) \sum_{n=1,2} [(d_n - \langle d \rangle) / \langle d \rangle]^2$ where $\langle d \rangle$ is the average bond length, increases substantially reducing the size of the rare earth. In the insulating phase $\Delta_d = 1.4 \times 10^{-6}$ for Pr, 1.6×10^{-5} for Sm, and 1.0×10^{-4} for Y, the value for Y being the average of $\Delta_d(\text{Ni1}) = 1.2[1] \times 10^{-4}$ and $\Delta_d(\text{Ni2}) = 0.8[1] \times 10^{-4}$ (in the metallic phase $\Delta_d = 1.4[2] \times 10^{-4}$). Namely, the static Jahn-Teller-like distortion of the octahedra is enhanced by 2 orders from Pr to Y ($\Delta_d = 3.3 \times 10^{-3}$ in LaMnO_3). The increase in the relative strength of the electron-lattice interaction is mainly due to the electronegativity increase along the 4f series that induces more ionic Ni-O bonds (at RT $\langle d(\text{Ni-O}) \rangle = 1.942$ and 1.959 Å for, respectively, Pr and Y).

The structural reorganization at T_{MI} gives rise to alternating contracted and expanded NiO_6 octahedra along the three directions of the crystal cell. Each distorted Ni1

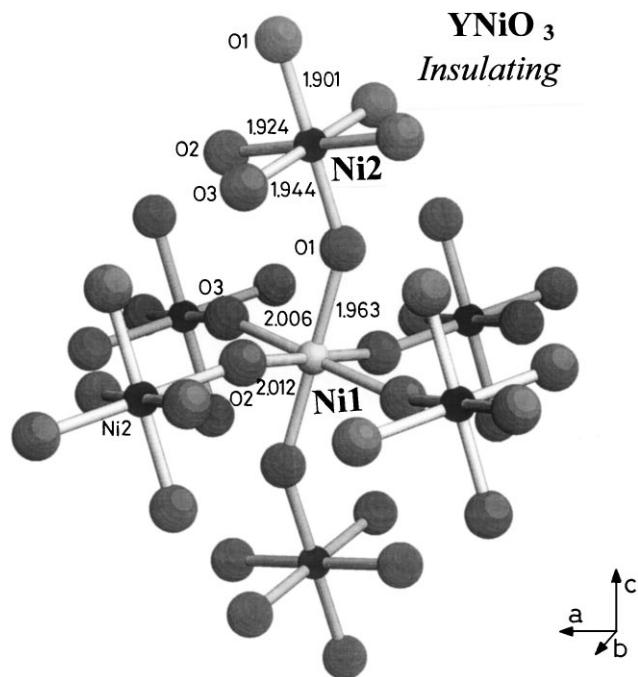


FIG. 3. Oxygen coordination for Ni1 and Ni2 in monoclinic YNiO_3 . Each Ni1O_6 shares corners with six Ni2O_6 octahedra, and vice versa.

octahedra ($\langle d(\text{Ni1-O}) \rangle = 1.994$ Å) shares its corners with six distorted Ni2 ones ($\langle d(\text{Ni2-O}) \rangle = 1.923$ Å). The phenomenological Brown's bond-valence model relates the bond length r_i and the valence s_i of a bond (for each central atom $v = \sum s_i$, $s_i = \exp[(r_0 - r_i)/B]$; $r_0 = 1.686$ for the $\text{Ni}^{3+}\text{-O}^{2-}$ pair) [17]. Using this approach, the calculated valences in the ionic limit are 2.62(1) and 3.17(1) for Ni1 and Ni2 cations, respectively. Consequently, the appearance of two alternating Ni states with $3 + \delta$, $3 - \delta'$ valences represents an important new element for the understanding of these oxides. This finding constitutes the first observation of a charge disproportionation phenomenon associated to the insulating phase of pure $R\text{NiO}_3$ perovskites. Although the ordered localization of breathing polarons has been reported in Ni^{2+} based $R_{2-x}\text{Sr}_x\text{NiO}_{4+y}$ oxides [18], it should be underlined that present Ni^{3+} oxides are stoichiometric and undoped. We are thus led to conclude that the occurrence of a charge disproportionation is the driving force for the orthorhombic-to-monoclinic transition concurrent with the charge localization at T_{MI} . A mutual self-doping process occurs at T_{MI} , in which a fraction of negative charge leaves the Ni2 octahedra and goes to neighboring Ni1 sites. Regarding the antibonding nature of the σ^* ($\text{O } 2p\text{-Ni } 3d$) bond, Ni1-O bonds expand (from $\langle d(\text{Ni1-O}) \rangle = 1.958$ to 1.994 Å) at the expense of the Ni2-O contraction (from $\langle d(\text{Ni2-O}) \rangle = 1.958$ to 1.923 Å). In other words, in the insulating phase each oxygen atom is linked through one short bond to a Ni2 and one long bond to a Ni1. A similar disproportionation was reported, for instance, for CaFeO_3 perovskite [19].

Finally, we shall focus on the magnetic structure. Neutron data in YNiO_3 reveal, below $T_N = 145$ K, the magnetic reflections shown in Fig. 4. Interestingly, the relative intensities of the magnetic reflections do not coincide exactly with those reported by some of us for Pr and Nd compounds [8]. The refinements of the magnetic structure using model 1 of Ref. [8] do not give a satisfactory agreement ($R_{\text{mag}} = 29\%$) in YNiO_3 . A complete charge disproportionation of the type $2\text{Ni}^{3+} \rightarrow \text{Ni}^{2+} + \text{Ni}^{4+}$ would lead to high-spin Ni^{2+} ($S = 1$) and diamagnetic Ni^{4+} (model 2 in Ref. [8]). In our case we expect an intermediate situation between model 1 and model 2 (see Fig. 4). A satisfactory fit of the magnetic intensities (considering the smallness of the magnetic peaks) was obtained for the collinear magnetic structure sketched in Fig. 4 ($R_{\text{mag}} = 15\%$). This magnetic structure is not uniquely determined by the present data, the proposed model being the most simple to explain the data. A noncollinear structure cannot be totally disregarded. As shown in Fig. 4, all magnetic moments lie in the a - c plane, deviated around $45^\circ (\pm 10^\circ)$ from the z axis. One of the main findings is that using this model the fit clearly converges to unequal moment values for the two Ni sites. The best magnetic fit corresponds to the moment values $1.4(1)$ and $0.7(1)\mu_B$ at, respectively, Ni1 and Ni2 sites, which implies an accumulation of extra electrons at the

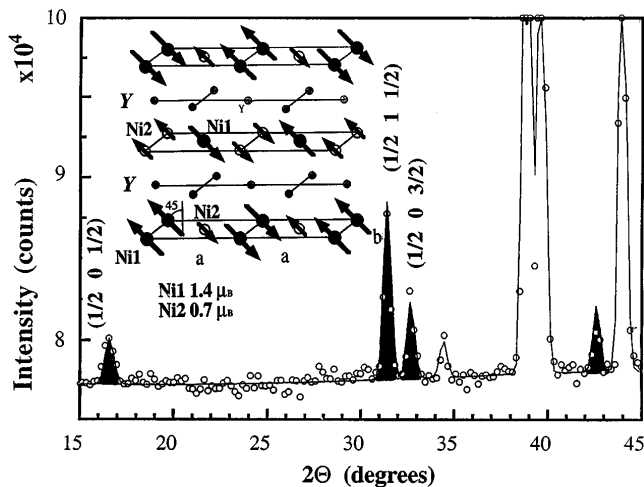


FIG. 4. Detail of the main magnetic reflections (shadowed) refined at 1.5 K. Inset: Magnetic ordering described in the text.

Ni1 sites at expenses of inducing charge defects at the adjacent Ni2 sites. The moment values along the three pseudocubic axes are successively $1 + \Delta m'$ [Ni1], $1 - \Delta m$ [Ni2], $-1 - \Delta m'$ [Ni1], and $-1 + \Delta m \mu_B$ [Ni2], with $\Delta m' \cong \Delta m \cong 0.35 \mu_B$. This suggests that the observed charges $(3 - \delta')$ [Ni1] and $(3 + \delta)$ [Ni2] correspond, indeed, to $\delta \cong \delta' \cong 0.35$. Moreover, regarding the fact that the Ni2 positions tend to a diamagnetic state, the Ni1-Ni1 magnetic interactions between second nearest neighbors are expected to be very significant compared with those between the nearest neighbors Ni1-Ni2 atoms. To this respect it is worth noticing that, consistently with the magnetic propagation vector, the coupling between Ni1 moments (second nearest neighbors) is AFM in the ac plane and FM parallel to the b axis.

In summary, we have reported the first observation of changes in the crystallographic symmetry at the metal-insulator transition in $R\text{NiO}_3$ perovskites. The single Ni site in the metallic phase of YNiO_3 breaks up into two sublattices at the gap opening. The insulating phase of this nickelate with enhanced electron-lattice coupling consists of expanded (Ni_1O_6) and contracted (Ni_2O_6) octahedra that alternate along the three directions of the crystal. The results show evidence for the stabilization of an uncompleted charge disproportionation, $2\text{Ni}^{3+} \rightarrow \text{Ni}^{2+} (S = 1) + \text{Ni}^{4+} (S = 0)$, associated with the MI transition. Below T_N the magnetic intensities are not identical to those

previously reported for less distorted $R\text{NiO}_3$ compounds, although they share the same magnetic propagation vector $\mathbf{k} = (\frac{1}{2}, 0, \frac{1}{2})$. Corroborating the charge disproportionation, unequal moments are found at Ni1 and Ni2 sites in the low temperature monoclinic phase. The magnetic interactions between second nearest neighbors (Ni1-Ni1) moments appear to be essential for the stabilization of the magnetic structure. These findings represent an important advance for the understanding of the charge localization in transition metal oxides with orbitally degenerated electrons.

The authors thank Dr. Eric Dooryhee for assistance during data collection on BM16, Professor E. Canadell and Dr. J. Rodríguez-Carvajal for fruitful discussions, and the ESRF and ILL for making available the beam time. Financial support by the OCYT-CYCyT (MAT97-0699, PB97-1181, PB97-1175 projects and funding the D1B CRG instrument). One of us (M.A.G.A.) thanks the Junta de Andalucía for Grant No. FQM-113.

- [1] P. Lacorre *et al.*, *J. Solid State Chem.* **91**, 225 (1991).
- [2] J.B. Torrance *et al.*, *Phys. Rev. B* **45**, 8209 (1992).
- [3] J.L. García-Muñoz *et al.*, *Phys. Rev. B* **46**, 4414 (1992).
- [4] J.B. Torrance *et al.*, *J. Solid State Chem.* **90**, 168 (1991).
- [5] M. Medarde *et al.*, *Phys. Rev. B* **46**, 14 975 (1992).
- [6] J.A. Alonso *et al.*, *J. Solid State Chem.* **120**, 170 (1995).
- [7] M. Medarde, *J. Phys. Condens. Matter* **9**, 1679 (1997).
- [8] J.L. García-Muñoz *et al.*, *Phys. Rev. B* **50**, 978 (1994).
- [9] J.L. García-Muñoz *et al.*, *Europhys. Lett.* **20**, 241 (1992).
- [10] J. Zaanen *et al.*, *Phys. Rev. Lett.* **55**, 418 (1985).
- [11] M. Medarde *et al.*, *Phys. Rev. Lett.* **80**, 2397 (1998).
- [12] J.A. Alonso *et al.* (to be published).
- [13] G. Démazeau *et al.*, *J. Solid State Chem.* **3**, 582 (1971).
- [14] A.C. Larson and R.B. von Dreele, Los Alamos National Laboratory Report No. LA-UR-86-748, 1994 (version: PC-98).
- [15] J. Rodríguez-Carvajal, *Physica (Amsterdam)* **192B**, 55 (1993).
- [16] J. Rodríguez-Carvajal *et al.*, *Phys. Rev. B* **57**, 456 (1998).
- [17] I.D. Brown, in *Structure and Bonding in Crystals*, edited by M. O'Keefe and A. Navrotsky (Academic Press, New York, 1981), Vol. 2, pp. 1-30; N.E. Brese *et al.*, *Acta Crystallogr. Sect. B* **47**, 192 (1991).
- [18] C.H. Chen *et al.*, *Phys. Rev. Lett.* **71**, 2461 (1993).
- [19] M. Takano *et al.*, *Phys. Rev. Lett.* **67**, 3267 (1991).